A two-stage photonic crystal fiber / silicon photonic wire short-wave infrared wavelength converter/amplifier based on a 1064 nm pump source

B. Kuyken,[1,2,*,†] F. Leo,[1,2,†] A. Mussot,[3] A. Kudlinski,[3] and G. Roelkens[1,2]

[1]*Photonics Research Group, Department of Information Technology, Ghent University-IMEC, Ghent B-9000 Belgium*

[2]*Center for Nano- and Biophotonics (NB-photonics), Ghent University, Belgium*

[3] *Université Lille 1, Laboratoire PhLAM, IRCICA, 59655 Villeneuve d'Ascq Cedex, France*

[†]*The authors contributed equally to this work*

**Bart.Kuyken@intec.ugent.be*

Abstract: We demonstrate a two-stage wavelength converter that uses compact near-infrared sources to amplify and convert short-wave infrared signals. The first stage consists of a photonic crystal fiber wavelength converter pumped by a Q-switched 1064 nm pump source, while the second stage consists of a silicon photonic wire waveguide wavelength converter. The system enables on-chip amplification and conversion of up to 30 dB . We demonstrate amplification in a broad wavelength range around 2344 nm using temporally long pulses (>300ps).

©2015 Optical Society of America

OCIS codes: (250.4390) Nonlinear optics, integrated optics; (190.4400) Nonlinear optics, materials; (190.3270) Kerr effect; (190.4380) Nonlinear optics, four-wave mixing.

References and links

1. M. Hochberg and T. Baehr-Jones, "Towards fabless silicon photonics," Nat. Photonics **4**(8), 492–494 (2010).
2. K. De Vos, I. Bartolozzi, E. Schacht, P. Bienstman, and R. Baets, "Silicon-on-Insulator microring resonator for sensitive and label-free biosensing," Opt. Express **15**(12), 7610–7615 (2007).
3. J. T. Robinson, L. Chen, and M. Lipson, "On-chip gas detection in silicon optical microcavities," Opt. Express **16**(6), 4296–4301 (2008).
4. J. G. Crowder, S. D. Smith, A. Vass, and J. Keddie, *Mid-Infrared Semiconductor Optoelectronics* (Springer-Verlag, 2006).
5. G. Roelkens, U. Dave, A. Gassenq, N. Hattasan, C. Hu, B. Kuyken, F. Leo, A. Malik, M. Muneeb, E. Ryckeboer, S. Uvin, Z. Hens, R. Baets, Y. Shimura, F. Gencarelli, B. Vincent, R. Loo, J. Van Campenhout, L. Cerutti, J.-B. Rodriguez, E. Tournié, X. Chen, M. Nedeljkovic, G. Mashanovich, L. Shen, N. Healy, A. C. Peacock, X. Liu, R. Osgood, and W. Green, "Silicon-based heterogeneous photonic integrated circuits for the mid-infrared," Opt. Mater. Express **3**(9), 1523 (2013).
6. M. N. Petrovich, F. Poletti, J. P. Wooler, A. M. Heidt, N. K. Baddela, Z. Li, D. R. Gray, R. Slavík, F. Parmigiani, N. V. Wheeler, J. R. Hayes, E. Numkam, L. Grűner-Nielsen, B. Pálsdóttir, R. Phelan, B. Kelly, J. O'Carroll, M. Becker, N. MacSuibhne, J. Zhao, F. C. Gunning, A. D. Ellis, P. Petropoulos, S. U. Alam, and D. J. Richardson, "Demonstration of amplified data transmission at 2 μm in a low-loss wide bandwidth hollow core photonic bandgap fiber," Opt. Express **21**(23), 28559–28569 (2013).
7. N. Hattasan, A. Gassenq, L. Cerutti, J.-B. Rodriguez, E. Tournie, and G. Roelkens, "Heterogeneous Integration of GaInAsSb p-i-n Photodiodes on a Silicon-on-Insulator Waveguide Circuit," IEEE Photon. Technol. Lett. **23**(23), 1760–1762 (2011).
8. G. Roelkens, U. Dave, A. Gassenq, N. Hattasan, C. Hu, B. Kuyken, F. Leo, A. Malik, M. Muneeb, E. Ryckeboer, D. Sanchez, S. Uvin, R. Wang, Z. Hens, R. Baets, Y. Shimura, F. Gencarelli, B. Vincent, R. Loo, J. V. Campenhout, L. Cerutti, J. Rodriguez, E. Tournie, X. Chen, M. Nedeljkovic, G. Mashanovich, L. Shen, N. Healy, A. C. Peacock, X. Liu, R. Osgood, and W. M. J. Green, "Silicon-based photonic integration beyond the telecommunication wavelength range," IEEE J. Sel. Top. Quantum Electron. **20**, 11 (2014).
9. B. Kuyken, X. Liu, R. M. Osgood, Jr., R. Baets, G. Roelkens, and W. M. Green, "Mid-infrared to telecom-band supercontinuum generation in highly nonlinear silicon-on-insulator wire waveguides," Opt. Express **19**(21), 20172–20181 (2011).

#234916 - $15.00 USD Received 18 Feb 2015; revised 4 May 2015; accepted 4 May 2015; published 8 May 2015
© 2015 OSA

10. D.D. Hudson, N. Singh, Y. Yu, C. Grillet, S. D. Jackson, A. Casas-Bedoya, A. Read, P. Atanackovic, S. G. Duval, S. Palombo, D. J. Moss, B. Luther-Davies, S. J. Madden, and B. J. Eggleton, "Octave spanning mid-IR supercontinuum generation in a silicon-on-sapphire waveguide" in Nonlinear Photonics, Barcelona, JTu6A (2014).
11. B. Kuyken, X. Liu, G. Roelkens, R. Baets, R. M. Osgood, Jr., and W. M. Green, "50 dB parametric on-chip gain in silicon photonic wires," Opt. Lett. **36**(22), 4401–4403 (2011).
12. X. Liu, B. Kuyken, G. Roelkens, R. Baets, R. M. Osgood, Jr., and W. M. Green, "Bridging the mid-infrared-to-telecom gap with silicon nanophotonic spectral translation," Nat. Photonics **6**(10), 667–671 (2012).
13. S. Zlatanovic, J. S. Park, S. Moro, J. M. C. Boggio, I. B. Divliansky, N. Alic, S. Mookherjea, and S. Radic, "Mid-infrared wavelength conversion in silicon waveguides using ultracompact telecom-band-derived pump source," Nat. Photonics **4**(8), 561–564 (2010).
14. R. K. Lau, M. Ménard, Y. Okawachi, M. A. Foster, A. C. Turner-Foster, R. Salem, M. Lipson, and A. L. Gaeta, "Continuous-wave mid-infrared frequency conversion in silicon nanowaveguides," Opt. Lett. **36**(7), 1263–1265 (2011).
15. Q. Lin, O. J. Painter, and G. P. Agrawal, "Nonlinear optical phenomena in silicon waveguides: modeling and applications," Opt. Express **15**(25), 16604–16644 (2007).
16. B. Kuyken, P. Verheyen, P. Tannouri, X. Liu, J. Van Campenhout, R. Baets, W. M. Green, and G. Roelkens, "Generation of 3.6 μm radiation and telecom-band amplification by four-wave mixing in a silicon waveguide with normal group velocity dispersion," Opt. Lett. **39**(6), 1349–1352 (2014).
17. A. Billat, S. Cordette, Y.-P. Tseng, S. Kharitonov, and C. S. Brès, "High-power parametric conversion from near-infrared to short-wave infrared," Opt. Express **22**(12), 14341–14347 (2014).
18. F. Gholami, B. P.-P. Kuo, S. Zlatanovic, N. Alic, and S. Radic, "Phase-preserving parametric wavelength conversion to SWIR band in highly nonlinear dispersion stabilized fiber," Opt. Express **21**(9), 11415–11424 (2013).
19. R. Soref, "Mid-infrared photonics in silicon and germanium," Nat. Photonics **4**(8), 495–497 (2010).
20. D. Nodop, C. Jauregui, D. Schimpf, J. Limpert, and A. Tünnermann, "Efficient high-power generation of visible and mid-infrared light by degenerate four-wave-mixing in a large-mode-area photonic-crystal fiber," Opt. Lett. **34**(22), 3499–3501 (2009).
21. M. E. Marhic, *Fiber Optical Parametric Amplifiers, Oscillators and Related Devices* (Cambridge University Press, 2008).
22. S. K. Selvaraja, P. Jaenen, W. Bogaerts, D. Van Thourhout, P. Dumon, and R. Baets, "Fabrication of photonic wire and crystal circuits in silicon-on-insulator using 193-nm optical lithography," J. Lightwave Technol. **27**(18), 4076–4083 (2009).
23. http://www.epixfab.eu/.
24. F. Leo, U. Dave, S. Keyvaninia, B. Kuyken, and G. Roelkens, "Measurement and tuning of the chromatic dispersion of a silicon photonic wire around the half band gap spectral region," Opt. Lett. **39**(3), 711-714 (2014).
25. N. Hattasan, B. Kuyken, F. Leo, E. Ryckeboer, D. Vermeulen, and G. Roelkens, "High-efficiency SOI fiber-to-chip grating couplers and low-loss waveguides for the short-wave infrared," IEEE Photon. Technol. Lett. **24**(17), 1536–1538 (2012).
26. X. Liu, R. M. Osgood, Y. Vlasov, and W. M. J. Green, "Mid-infrared optical parametric amplifier using silicon nanophotonic waveguides," Nat. Photonics **4**(8), 557–560 (2010).

1. Introduction

The CMOS compatible silicon-on-insulator (SOI) platform has over the last years developed as the waveguide platform of choice for optical interconnect applications [1]. More recently new applications, in particular sensing applications such as bio-molecule detection [2] and gas sensing [3], have fueled the SOI platform development further. For such applications, it can be beneficial to step away from the telecom wavelength range and move towards the short-wave infrared and mid-infrared wavelength region. In these wavelength regions, many molecules have strong and well-defined absorption lines [4]. Silicon photonic chips operating in this wavelength range could unlock this enormous potential for sensing and lead to a whole new class of very sensitive and selective sensors [5]. Besides for optical sensing applications, the short-wave infrared (>2.0um) wavelength range is also being considered for future telecommunication systems [6]. Although it is possible to heterogeneously integrate III-V epitaxial layers [7, 8] on silicon to provide gain to the passive silicon circuit, it is hard to integrate a widely tunable short-wave infrared or mid-infrared source on a silicon chip due to the limited gain bandwidth of III-V semiconductor structures. We have shown before that the combination of the high nonlinear refractive index of silicon, the strong confinement in silicon photonic wires and the absence of two photon absorption in silicon beyond ~2200 nm

#234916 - $15.00 USD Received 18 Feb 2015; revised 4 May 2015; accepted 4 May 2015; published 8 May 2015
© 2015 OSA

enables efficient nonlinear processes when the silicon waveguides are pumped at short-wave infrared wavelengths. Indeed, supercontinuum generation [9, 10], parametric amplification [11] and wavelength translation [12] of signals have been demonstrated. However, the main limitation of implementing these functionalities in a real system at the moment is that very complex pump sources are often needed. Most experiments use short picosecond pump pulses coming from an expensive and bulky optical parametric oscillator. Although there have been experiments demonstrating four wave mixing in silicon waveguides with longer (ns) pulses [13] and continuous wave sources [14] the conversion efficiency has been relatively low, of the order of −20 dB in the short-wave infrared, and requires quite complex setups. Furthermore in these previous results pump sources around 1950-2025 nm are used. In this wavelength region there is still significant two-photon absorption such that gain cannot be obtained for long pump pulses because of the free carrier absorption [15].

In this paper we demonstrate a simple two-stage short-wave infrared wavelength converter/amplifier only involving a 1064nm microchip laser and a continuous wave 688nm laser diode. The first stage consists of a photonic crystal fiber (PCF), generating a pump pulse at 2345nm used in the second conversion stage, realized using a silicon photonic waveguide. The two-stage amplifier is able to convert long pulses (>300 ps pulses) with a very high efficiency (up to 30dB maximum gain) over a broad wavelength band ranging from 2275 nm up to 2325 nm. This result becomes only possible by generating a pump well beyond the two-photon absorption band gap of silicon (2200 nm) such that two-photon absorption and free carrier absorption are suppressed.

To the best of our knowledge, this represents the first amplification of quasi-CW pulses in a silicon chip with net off-chip gain. We believe our results can impact both signal processing and infrared spectroscopy applications. Such a two-stage converter/amplifier could allow for all-optical signal processing of data-packets for future telecommunication systems operating in the 2 μm wavelength range. Moreover, through further dispersion engineering of the silicon waveguide [16], this technique could be used to amplify telecom band signals in a silicon waveguide in the long pulse (or CW) regime. Furthermore, in contrast to highly nonlinear silica fibers where conversion of light to a band around 2000 nm was shown [17, 18], silicon waveguides could allow to generate light deeper into the mid-infrared given the transparency of the silicon-on-insulator platform up to about 4.0 μm [19]. In that case, further dispersion engineering [20] and an additional cheap near infrared diode laser as a seed for the second conversion stage would allow to generate mid-infrared light in the fingerprint wavelength region (>3um).

#234916 - $15.00 USD Received 18 Feb 2015; revised 4 May 2015; accepted 4 May 2015; published 8 May 2015
© 2015 OSA

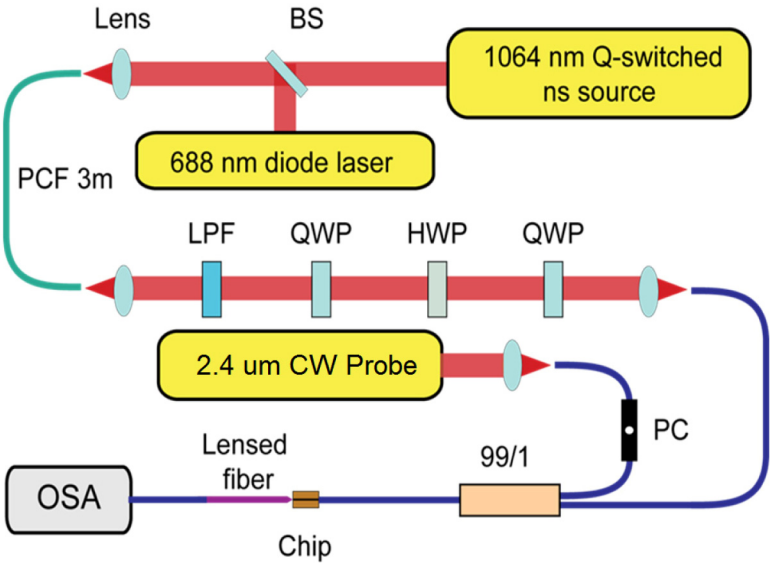

Fig. 1. A schematic of the two-stage wavelength converter/amplifier. The first stage, the photonic crystal fiber, is pumped by a low-cost 1064nm Q-switched laser and seeded by a low-cost visible laser at 688 nm. The second stage consists of a silicon photonic wire waveguide.

2. Two-stage wavelength converter/amplifier

The schematic of the two-stage wavelength converter/amplifier setup is shown in Fig. 1. In the first stage, the frequency conversion is realized using a PCF, while in the second stage a silicon photonic waveguide is used. In both waveguides the degenerate four-wave mixing process is used to convert two pump photons in one idler and one signal photon.

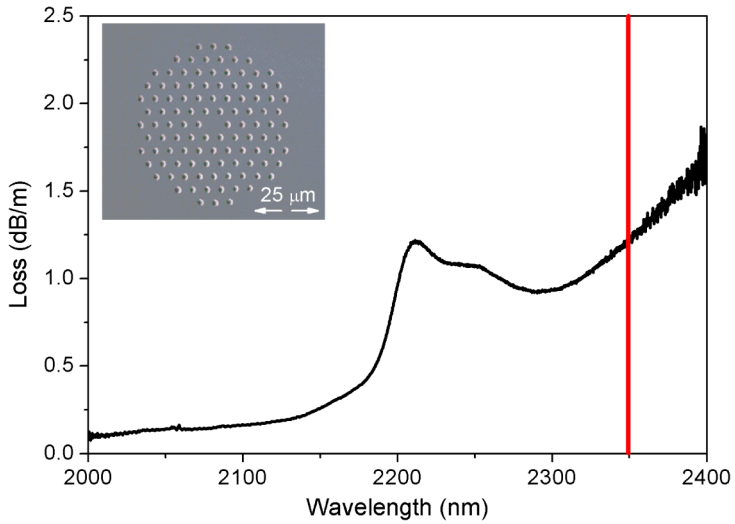

Fig. 2. The linear propagation loss of the PCF. The red line indicates the wavelength that is generated through degenerate four-wave mixing in the PCF. The inset shows a SEM picture of the cross-section of the used PCF.

In the first stage a 1064 nm Q-switched microchip laser acts as a pump in the PCF to generate an idler around 2345nm that will serve as a pump in the second silicon waveguide

#234916 - $15.00 USD Received 18 Feb 2015; revised 4 May 2015; accepted 4 May 2015; published 8 May 2015
© 2015 OSA

stage. This wavelength has been chosen because it is well beyond the half band gap of silicon, while at the same time, having acceptable propagation loss in the PCF. The dispersion of the PCF has been adjusted by controlling the relative air hole diameter sizes in order to achieve a perfect phase matching around 2345 nm by pumping at 1064 nm. The cross-section of the fiber is shown in the inset of Fig. 2. The pitch and diameter of the air holes are respectively 5.6 μm and 2.08 μm leading to a zero dispersion wavelength of 1174 nm. By pumping at 1064 nm, the standard phase matching relation using dispersion terms up to the sixth order [20] predicts a perfect phase matching at 688 nm and 2344 nm. The PCF length has been optimized to 3 m in order to obtain the maximum power on the idler wave. The linear attenuation has been obtained through a cutback measurement on a longer sample of 10 m of fiber and is shown in Fig. 2. The loss is less than 2 dB/m between 2000 nm and 2400 nm, where the idler wave is generated. This value is low enough to not affect the FWM process significantly. The pulse duration of the Q-switched laser located at 1064 nm is 600 ps and the repetition rate is 6.5 kHz. The coupled peak power of the pump pulses inside the PCF has been estimated to be 4.3 kW. A continuous-wave laser seed of ~100 μW at 688 nm (the signal wavelength) is combined with the pump pulses and coupled into the PCF to seed the four-wave mixing process in order to ensure that the generated short-wave infrared idler pulses have a clean temporal profile. The output of the PCF is collimated and coupled into a SMF-28 fiber as shown in Fig. 1. In the free space path, a filter blocks the remaining 1064 nm pump light as well as the 688 nm seed, and the polarization of the beam is adjusted to excite the TE mode of the silicon photonic waveguide.

The spectrum of the generated pulse recorded with a 1 nm resolution short-wave infrared optical spectrum analyzer is shown in the left panel of Fig. 3. It is centered at 2344 nm in excellent agreement with the prediction provided by the phase matching relation. Its duration is estimated by measuring the pulse duration of the signal pulse generated at 688 nm with a 12 GHz photodiode. Due to the symmetric nature of the degenerate four-wave mixing process this is equivalent to measuring the pulse width of the idler pulse [21]. The oscilloscope trace of the signal is shown in the right panel of Fig. 3. The full width at half maximum of the pulse is measured to be 326 ps. This is shorter than the pump pulse, because the conversion efficiency is exponentially dependent on the instantaneous power of the pump pulse [21]. The shape of the idler pulse gets transformed by this nonlinear operation.

The second stage of the amplifier consists out of a dispersion engineered silicon-on-insulator waveguide. The photonic wire is fabricated in a CMOS pilot line [22, 23] on a 200 mm silicon-on-insulator (SOI) wafer, consisting of a 220 nm silicon waveguide layer on top of a 2 μm buried oxide layer. The 7 cm-long air-clad photonic wire has a rectangular cross-section of 890 nm x 220 nm. In a post-processing step the waveguides where slightly underetched by partially removing the silicondioxide in a 1% HF solution. The partial underetching of the waveguides allows further engineering of the dispersion of the waveguides [24]. In the inset of Fig. 4, a bird's eye view of the waveguide is presented. Due to the partial HF underetch, the waveguide can be seen standing on a 140 nm tall pillar. The dispersion of the waveguide used here was simulated to be −1.17 ps^2/m at 2345nm (TE polarization). A 1 dB/cm waveguide loss was measured in a cut-back measurement on 1, 2, 4 and 7 cm long waveguides. The waveguide was terminated with a grating coupler [25] at one side and cleaved at the other side. The grating coupler efficiency was found to be −8.5 dB at the pump wavelength.

#234916 - $15.00 USD Received 18 Feb 2015; revised 4 May 2015; accepted 4 May 2015; published 8 May 2015
© 2015 OSA

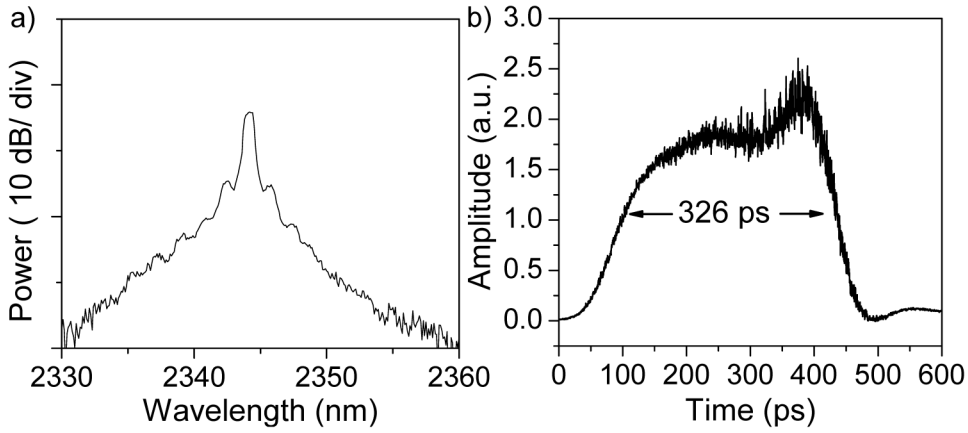

Fig. 3. a) The optical spectrum of the short-wave infrared pulse generated in the PCF. b) The time-domain trace of the generated visible pulse at 688 nm in the PCF, which is a good indicator for the time-domain trace of the generated short-wave infrared pulse.

In order to assess the performance of the two-stage converter/amplifier, the short-wave infrared pulses generated in the first stage converter stage are combined with a probe laser in a 99/1 fiber coupler. For this assessment a continuous wave OPO was used. The insertion loss of the coupler is 3 dB in the 2300 nm to 2400 nm wavelength range. The coupled average power of the short-wave infrared pulse train in the SMF-28 fiber is measured to be 100 µW. The calculated peak power, assuming a pulse duration of 300 ps, is therefore 40 W before the 99/1 splitter. The pulse peak power inside the silicon waveguide is 2.8 W. The continuous wave on-chip power of the seed laser was well below 100 µW.

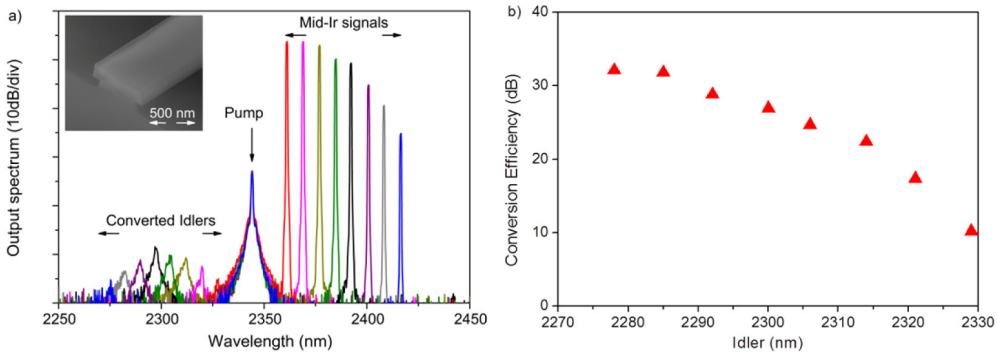

Fig. 4. The output spectrum and the on-chip net conversion efficiency of the two-stage wavelength converter/amplifier. Fig. a) shows the output spectrum for a set of different continuous wave seeding signals. The pump centered around 2344 nm converts the continuous wave signals to a (pulsed) converted idler. Fig. b) shows on-chip net conversion efficiency as a function of the idler wavelength.

The output spectrum after the waveguide for different short-wave infrared seed wavelengths is shown in Fig. 4(a). The conversion efficiency can be calculated as in [26] by correcting for the duty cycle of the pump pulse train. Figure 4 b) shows the conversion efficiency as a function of the seed wavelength. The efficiency was calculated after taking in account the the duty cycle of the Q-switched laser. As can be seen in the figure, the net on-chip conversion efficiency reaches up to 32 dB and conversion is established over a wide bandwidth. As such we are able to achieve for the first time net-gain for long pulses in a silicon waveguide. The conversion bandwidth is in this experiment limited by the bandwidth of the grating coupler used to interface with the silicon chip.

#234916 - $15.00 USD Received 18 Feb 2015; revised 4 May 2015; accepted 4 May 2015; published 8 May 2015
© 2015 OSA

3. Conclusion

In conclusion, we have demonstrated the efficient conversion of long (>300ps) short-wave infrared pulses in a two-stage wavelength converter / amplifier with over 30 dB net on-chip conversion efficiency. The setup consists of a compact silicon waveguide and standard pure silica PCF as well as small and low-cost sources used for generating the pump for the silicon waveguide converter/amplifier stage. Through further dispersion engineering of the silicon waveguide [14], the continuous wave optical parametric oscillator that was used in this proof-of-principle experiment could be replaced by cheap near-infrared laser sources allowing downconversion further into the mid-infrared.

We believe our results highlight the potential of combining silica fiber and silicon waveguides for nonlinear optics using pump sources around 2.3 um where the low linear losses of the silica PCF and the low nonlinear losses of the silicon waveguide allow for efficient four-wave mixing.

Acknowledgments

This work was supported by the FP7-ERC-MIRACLE and FP7-ERC-InSpectra project, the "Fonds Européen de Développement Economique Régional", the Labex CEMPI (ANR-11-LABX-0007) and Equipex FLUX (ANR-11-EQPX-0017) through the "Programme Investissements d'Avenir". Bart Kuyken would like to acknowledge the Special Research Fund (BOF) for providing a post-doctoral grant. We would like to acknowledge Prof. Johan Bauwelinck for the use of a fast photodiode.

#234916 - $15.00 USD Received 18 Feb 2015; revised 4 May 2015; accepted 4 May 2015; published 8 May 2015
© 2015 OSA